ARTICLE NO. 79-0123R

G80-054

Semianalytic Theory for a Close-Earth Artificial Satellite

0005

J.J.F. Liu*
Headquarters Aerospace Defense Command, Peterson Air Force Base, Colo.
and
R.L. Alford†
Northrop Services, Inc., Huntsville, Ala.

A semianalytical method is used to estimate the decay history/lifetime and to generate orbital ephemerides for close-Earth satellites perturbed by atmospheric drag and by Earth oblateness due to the spherical harmonics J_2, J_3, and J_4. The theory is developed through the use of a method of averaging and employs sufficient numerical emphasis to include a rather sophisticated atmospheric density model. The averaged drag effects with respect to mean anomaly are evaluated by a Gauss-Legendre quadrature, while the averaged variational equations of motion are integrated numerically with automatic step size and error control. Proper transformations, initialization procedures, and numerical results are also given.

Introduction

THIS paper presents the pertinent aspects of a semianalytic theory developed to estimate the decay history/lifetime (long-term prediction) and generate short-term orbital ephemerides for close-Earth artificial satellites perturbed by atmospheric drag and Earth oblateness. Although there are analytical solutions which describe the effects of atmospheric drag on the motion of an artificial satellite in the gravitational field of an oblate Earth, these solutions are usually based on simplified analytical models for the atmospheric density. Brouwer and Hori[1] used the Von Zeipel method and an exponential density model to obtain their solutions. Lane[2] introduced the power function density model[3] to develop a coupled solution through the use of the same method used by Brouwer and Hori. By adopting a power function density model, Lane was able to integrate the equations of motion without expanding the density function in a series and thus avoided the associated convergence problem for low perigee heights. Later, Lane and Cranford[4] extended Lane's previous theory to avoid the singularities. Recently, Hoots[5] adopted Brouwer's drag-free solution[6] with Lyddane's modification[7] and the power function density model to derive a coupled analytic solution using a method of averaging. Zee[8] used an asymptotic method and an exponential density function model to develop a closed-form solution in spherical coordinates. It should be noted that Zee included only the second harmonic of the oblateness of the Earth and the other theories included second through fourth harmonics. For all of the theories cited above, a nonrotating, static, and spherical atmospheric density model was assumed. To improve the density model, Chen[9] introduced a modified exponential function which exhibited the characteristics of atmospheric oblateness and diurnal bulge and arrived at an analytic solution using a two-variable asymptotic expansion method. In his solution, the drag effects are assumed to be second order in magnitude. More recently, Mueller[10] developed an analytic density representation which requires ten parameters to be calibrated for a specific density model. He then used a Fourier series expansion of the analytic representation for drag, certain recursive formulas for higher-order geopotential functions, and an averaging technique to obtain a solution in terms of Poincaré-similar orbital elements.[11] To maintain accuracy, it may be required to recalibrate the ten fitting parameters periodically. It should also be noted that most of the analytic theories mentioned here have some limitations on the size of the eccentricity and/or the perigee height due to the use of series expansions.

An alternative approach to account for the effects of atmospheric drag on the motion of artificial satellites in the presence of the gravitational field of an oblate Earth is to adopt a combination of general and special perturbation techniques. Such an approach, as it will be presented in this paper, is often referred to as a semianalytic method. This method enhances efficiency through the use of analytical techniques and makes use of sufficient numerical methods to permit the inclusion of a state-of-the-art atmospheric density model without using series expansions. Pimm[12] developed a semianalytic long-term orbit generator which used Simpson's method to evaluate the averaged drag effects. He utilized one of several available density models on a set of smoothed orbital elements[13] and then numerically integrated the smoothed equations of motion. Kaufman and Dasenbrock[14] also developed a semianalytic long-term orbit generator for planetary orbiters using quadrature techniques to evaluate the averaged drag effects for a nonrotating atmosphere. Both of the semianalytic theories just mentioned emphasize the long-term predictions, since precise integration of the fast variable, mean anomaly, are not included. Cefola et al[15] used a method of averaging and recursive formulas to obtain the averaged equations of motion due to higher-order geopotential functions, third-body effects, and solar radiation pressure in terms of equinoctial orbital elements. Recently, McClain et al.[16] extended and used the same technique and developed a hybrid averaged orbit generator to include the drag effects. These authors used quadrature techniques to evaluate the drag effects and numerically integrated the averaged equations of motions. However, many detail analyses and the numerical examination for high-drag test cases were not given. To analyze the motion of a deep-space object, Hujsak simplified and extended the Lane and Cranford theory[4] to include third-body point mass effects and some chosen tesseral and sectoral harmonics using a method of averaging to obtain an essentially analytical solution. For the drag-free analysis associated with his theory, the reader is referred to Ref. 17.

A system of six first-order ordinary differential equations for a set of well-defined mean orbital elements[18] derived by a method of averaging, which describes the motion of an ar-

Presented as Paper 79-0123 at the AIAA 17th Aerospace Sciences Meeting, New Orleans, La., Jan. 15-17, 1979; submitted Feb. 16, 1979; revision received Feb. 4, 1980. This paper is declared a work of the U.S. Government and therefore is in the public domain.

Index category: Earth-Orbital Trajectories.

*Mathematician, Office of Astrodynamics. Member AIAA.

†Presently, Senior Lead Engineer, Honeywell, Inc., Minneapolis, Minn. Member AIAA.

tificial satellite perturbed by the second through the fourth harmonics of the geopotential function, is extended to include the drag effects of a rotating atmosphere described by a Jacchia density model (1970). For most close-Earth, low-altitude satellites with small eccentricities, the perturbations due to other forces (e.g., solar-lunar effects, solar radiation pressure, higher-order geopotential perturbations, etc.) are usually smaller than the effects caused by the basic uncertainties in our knowledge of atmospheric density and the associated drag coefficient. Consequently, these additional perturbations are not included in the present study. Due to the complexity of the density evaluation from the Jacchia model, the analytical expressions for the averaged drag effects become difficult if not impossible to obtain through the use of series expansions and model simplifications. To maintain the density model accuracy, the averaged drag effects are evaluated numerically by a Gauss-Legendre quadrature.[19] The averaged variational equations of motion in which the right-hand side of the equations are free from the fast varying mean anomaly are then integrated numerically with a much larger step size than those normally used in special perturbation techniques. This development of an efficient and useful orbital decay model is based on the use of the transformation derived by Liu[18] which permits the system of differential equations for the osculating state to be transformed into a system for propagation of the mean state. Treating the mean or averaged equations allows one to avoid the numerical inefficiencies created by the fast dynamical variations with periods on the order of one orbit.

There is a fundamental difficulty in predicting the orbital motion of a satellite due to the fact that several characteristics of the satellite and atmosphere are not deterministically known. This difficulty not only makes it necessary to perhaps specify orbital predictions in a probabilistic way, but also complicates the process of verification for any proposed decay model. Thus, comparisons of predicted satellite decay vs actual observed data may reveal deviations which could be attributed to an inadequate deterministic model, noisy tracking data, or expected deviations in the stochastic variables associated with the prediction problem (e.g., ballistic coefficient, sunspot number, and geomagnetic activity). Therefore, to avoid this difficulty, the predictions generated by this theory have been examined and compared with the numerical integration of the original equations of motion for the osculating state assuming deterministic or known values for the random variables in the model. This parametric analysis is accomplished with the aid of two independent numerical integration programs using an identical atmospheric density model and gravitational potential representation. Proper initialization procedures which are vital to the prediction accuracy are discussed and the results of the numerical comparison have exhibited excellent accuracy as well as large savings in computer time.

Although some perturbative effects are ignored, as discussed earlier, it is believed that a priori uncertainties in atmospheric densities and the ballistic coefficient generally have a larger impact on prediction accuracies for a low-altitude artificial satellite. On the other hand, if there is any specific significant perturbative force which needs to be included, the formulation of this theory is in an ideal form for further extension.

A major portion of the work presented in this paper was originally accomplished in 1974 without the inclusion of the fast variable (mean anomaly) in the integration to study the long-term prediction.[20] The theory has since been extended to obtain a semianalytic solution for all six orbital elements.

Equations of Motion

The equations of motion, for a close-Earth artificial satellite perturbed by the Earth's oblateness and atmospheric resistance are well known and will be given here without derivation. The set of equations used in this paper are those derived in Ref. 21. The subscripts G and D are used to designate the perturbing terms due to the Earth's oblateness and the atmospheric drag, respectively. The equations of motion associated with the semimajor axis a, eccentricity e, inclination i, ascending node Ω, argument of perigee ω, and mean anomaly M take the form

$$\dot{x}_j = (\dot{x}_j)_G + (\dot{x}_j)_D \qquad (j=1,2,\ldots 6) \tag{1}$$

where $\{x_j\} = (a,e,i,\Omega,\omega,M\}$ with initial conditions $(x_j)_0$. In formulating Eqs. (1), it has been assumed that the satellite moves in an elliptical orbit‡ about an axially symmetric Earth (only the second, third, and fourth spherical harmonics are included in the analysis), and the resultant atmospheric drag force per unit mass is taken as $\frac{1}{2}B\rho V^2$, whereas the aerodynamic lift is ignored. Here the notations B, ρ, and V are used to designate the ballistic coefficient, air density, and satellite speed relative to the ambient air, respectively. To assist in later discussions, the drag-perturbing terms are given here for reference. They are

$$\begin{aligned}
(\dot{a})_D &= -B\rho V\frac{a}{1-e^2}\left[1+e^2+2e\cos f - \omega_a\frac{\sqrt{a^3(1-e^2)^3}\cos i}{\sqrt{\mu}}\right]\\
(\dot{e})_D &= -\tfrac{1}{2}B\rho V\left\{2(e+\cos f) - \omega_a\frac{r^2\cos i}{\sqrt{\mu a(1-e^2)}}\left[2(e+\cos f) - e\sin^2 f\right]\right\}\\
(\dot{i})_D &= -\tfrac{1}{2}\,B\rho V\frac{r^2\omega_a}{\sqrt{\mu a(1-e^2)}}\sin i\cos^2 u\\
(\dot{\Omega})_D &= \tfrac{1}{2}B\rho V\frac{r^2\omega_a}{\sqrt{\mu a(1-e^2)}}\sin u\cos u\\
(\dot{\omega})_D &= \tfrac{1}{2}B\rho V\frac{\sin f}{e}\left[2-\frac{r^2\omega_a\cos i}{\sqrt{\mu a(1-e)^2}}(2+e\cos f)\right]\\
(\dot{M})_D &= -\tfrac{1}{2}B\rho V\left[2e\sin E+\frac{2}{e}\sqrt{1-e^2}\sin f - \frac{r^2\omega_a\cos i}{e\sqrt{\mu a}}\sin f(2+e\cos f)\right]
\end{aligned} \tag{2}$$

The notations f, E, u, r, ω_a, and μ stand for true anomaly, eccentric anomaly, argument of latitude, magnitude of position vector, atmospheric rotational speed, and the product of the gravitational constant and the mass of Earth, respectively.

Transformation and the Averaged Equations of Motion

A general perturbation theory, namely the method of averaging, will be used here to obtain a set of averaged variational equations which describes the averaged motion of the dynamical system, Eqs. (1). Without rigorous proof, it is assumed that the drag-perturbing terms appearing in the right-hand members of Eqs. (2) also satisfy the conditions required by the method of averaging.[22,23] Again, only the results of the associated transformation and the averaged dynamical system will be given. The related analysis can be found in Ref. 18.

Since the dynamical system, Eqs. (1), is nonlinear in nature and complex in form, additional assumptions are made in this

‡The singularities at $e=0$ and $i=0$ can be taken care of by introducing new orbital elements.

paper to produce an analytically manageable system. These assumptions are:

1) J_2 is a first-order quantity.
2) J_3, J_4 are second-order quantities.
3) Drag perturbations are second-order effects. (Discussions concerning this assumption are given in Ref. 24.)
4) The atmospheric rotational speed is of the same order of magnitude as that of the Earth.
5) The ballistic coefficient is a constant parameter.

Here J_2, J_3, and J_4 are the coefficients of the second, third, and fourth harmonics of the oblateness of the Earth.

By assuming that the drag effects are second order, the first-order transformation from the osculating orbital elements a, e, i, Ω, ω, M to the averged elements a_m, e_m, i_m, Ω_m, ω_m, and M_m is the same as in the drag-free problem. It is

$$x_j = x_{jm} + x_{jsp}(a_m, e_m, i_m, \omega_m, M_m) \qquad (j = 1,2,\ldots 6)$$
$$r = r_m + r_{sp}(a_m, e_m, i_m, \omega_m, M_m) \qquad (3)$$

where the subscripts m and sp stand for the corresponding averaged value and the short-periodic variation for the designated orbital element, respectively. The additional transformation for the magnitude of the position vector r is included here for the reason that to recover the important J_2-drag coupled effects, the instantaneous altitude is required. It is important to note that the expressions in the right-hand members of the transformation are functions of the averaged orbital elements only. The transformed (or averaged) dynamical system has the form

$$\begin{aligned} \dot{a}_m &= \langle \dot{a}_D \rangle & \dot{\Omega}_m &= \langle \dot{\Omega}_G \rangle + \langle \dot{\Omega}_D \rangle \\ \dot{e}_m &= \langle \dot{e}_G \rangle + \langle \dot{e}_D \rangle & \dot{\omega}_m &= \langle \dot{\omega}_G \rangle + \langle \dot{\omega}_D \rangle \\ (\dot{i}_m) &= \langle (\dot{i}_G) \rangle + \langle (\dot{i}_D) \rangle & \dot{M}_m &= \langle \dot{M}_G \rangle + \langle \dot{M}_D \rangle \end{aligned} \qquad (4)$$

where the symbol $\langle F \rangle$ stands for the averaged value of F with respect to mean anomaly. The initial conditions, a_{m0}, e_{m0}, i_{m0}, Ω_{m0}, ω_{m0}, and M_{m0}, which remain to be determined, will be discussed in the latter part of this paper. The explicit expressions for a_{sp}, e_{sp}, i_{sp}, Ω_{sp}, ω_{sp}, M_{sp}, r_{sp} and $\langle \dot{a}_G \rangle$, $\langle \dot{e}_G \rangle$, $\langle (\dot{i}_G) \rangle$, $\langle \dot{\Omega}_G \rangle$, $\langle \dot{\omega}_G \rangle$, $\langle \dot{M}_G \rangle$ are given in Appendixes A and B, respectively. By assuming that the drag effects are second-order quantities, we have

$$\langle \dot{x}_D \rangle = \frac{1}{2\pi} \int_0^{2\pi} \dot{x}_D(a_m, e_m, i_m, \omega_m, M)\, dM \qquad (5)$$

where x stands for any one of the six orbital elements. Up to this point, the analysis remains totally analytic with an unspecified atmospheric density model. By choosing a simplified density model which makes the equations of motion tractable, the right-hand members of Eq. (5) may be integrated to obtain analytical averaged equations of motion. For a rather sophisticated density function, such as Jacchia's model, a numerical evaluation of these integrals may be the most feasible and realistic approach to estimate the drag effects. The latter approach will be discussed in the following sections to include the use of a modified Jacchia 1970 density model.

Simplified Averaged Equations of Motion

Theoretically, we can evaluate the integrals in Eq. (5) numerically without simplification. For computer efficiency, some of the less significant integrals will be ignored. For close-Earth satellites, we will assume that the principal drag effects are $\dot{a}_D$, $\dot{e}_D$, and the remaining effects are insignificant. Furthermore, it is also noted that the expression $\langle (\dot{i}_G) \rangle$ is second order in magnitude and has a multiplier e or e^2; therefore, i_m is assumed to be constant to save computation. With these additional assumptions, the simplified averaged equations of motion become

$$\begin{aligned} \dot{a}_m &= \langle \dot{a}_D \rangle & \dot{\Omega}_m &= \langle \dot{\Omega}_G \rangle \\ \dot{e}_m &= \langle \dot{e}_G \rangle + \langle \dot{e}_D \rangle & \dot{\omega}_m &= \langle \dot{\omega}_G \rangle \\ (\dot{i}_m) &= 0 & \dot{M}_m &= \langle \dot{M}_G \rangle \end{aligned} \qquad (6)$$

where

$$\langle \dot{a}_D \rangle = -\frac{1}{2\pi} \int_0^{2\pi} B\rho V \frac{a}{1-e^2} \left[1 + e^2 + 2e\cos f - \omega_a \cos i \sqrt{\frac{a^3(1-e^2)^3}{\mu}} \right] dM$$

$$\langle \dot{e}_D \rangle = -\frac{1}{2\pi} \int_0^{2\pi} B\rho V \left\{ e + \cos f - \frac{r^2 \omega_a \cos i}{2\sqrt{\mu a(1-e^2)}} [2(e+\cos f) - e\sin^2 f] \right\} dM \qquad (7)$$

with the same initial conditions. The integrations, which give the averaged drag effects with respect to M from 0 to 2π, will be carried out with respect to the true anomaly f instead of the mean anomaly M, through the transformation

$$dM = (r/a)^2 (1-e^2)^{-1/2} df \qquad (8)$$

The explicit expressions for B and V have the form

$$B = C_D A / M_s$$

$$V = \left[\frac{\mu}{p} (1 + e^2 + 2e\cos f) \right]^{1/2} \left[1 - \frac{(1-e^2)^{3/2}}{1 + e^2 + 2e\cos f} \frac{\omega_a}{n} \cos i \right] \qquad (9)$$

Atmospheric Density Model

The atmospheric density ρ shall be regarded as empirically given since there is, in general, no complete analytical expression available. On the other hand, the density function ρ can be written in several different forms (see Refs. 1, 5, 8, and 9) so that analytical solutions within certain specified accuracies can be obtained through several perturbation techniques. However, in order to insure the accuracy desired in this analysis, the density function is adopted from the 1970 MSFC model,[25] with some programming modifications. This model is a modified version of the 1970 Jacchia atmospheric density model.[26]

To use the Jacchia density model for ephemeris prediction, values for daily 10.7 cm solar flux ($F_{10.7}$), mean solar flux ($\bar{F}_{10.7}$), and geomagnetic index (a_p) are required parameters as functions of time. It should be noted that these predicted values are usually associated with substantial uncertainties and the accurate values for solar fluxes and a_p are generally not available for long-term prediction.

Numerical Techniques

The solution of the equations of motion, Eqs. (6), requires the numerical evaluation of a system of ordinary differential equations with respect to the independent variable time. To calculate the derivatives for a given time, Gauss-Legendre quadrature is used with respect to true anomaly. Thus the numerical analyses employed in this theory can be divided into two separate parts, each having its own error control. The error control for the differential equations will decide the time step, and the quadrature error control will determine the order of the quadrature evaluation. For details, the reader is referred to Ref. 24.

Initialization

The approach discussed in the previous sections may be used to study the long-term predictions and generate short-term ephemerides for a close-Earth artificial satellite provided that proper transformation and initialization procedures are used.

Given the initial conditions for the osculating orbital elements a_0, e_0, i_0, Ω_0, ω_0, and M_0, the associated averaged elements a_{m0}, e_{m0}, i_{m0}, Ω_{m0}, ω_{m0}, and M_{m0} can be evaluated explicitly from the transformation, Eqs. (3), by iteration. Since the transformation is of the first order in J_2, the initial conditions for the averaged orbital elements and the averaged mean motion are accurate to the same order of magnitude. Therefore, it is well known that the theory will exhibit a second-order secular mean anomaly (in-track) error due to the initialization procedure. This fact has been demonstratred by Lyddane and Cohen[27] by recovering the second-order quantities due to J_2^2 in semimajor axis. Later, Breakwell and Vagners[28] also investigated the problem and concluded that the in-track accuracy may be kept to the second order by either calibrating the mean motion with the aid of the energy integral or fitting an orbit theory to data over many revolutions.

In the current analysis, the second-order quantities in the transformation equations are not included. For long-term predictions, as compared with those from a numerical integration program with a known ballistic coefficient, the in-track accuracy may not be of primary interest, and the first-order transformation, Eqs. (3), can be used in the initialization procedure with reasonable accuracy. On the other hand, for use in short-term ephemerides generation, the orbit theory should be fitted to the orbital data over many revolutions to determine the initial conditions as well as a suitable ballistic coefficient for accurate prediction.

Numerical Results

As discussed in the previous section concerning initialization procedures, the numerical results will be presented in two parts.

Long-Term Prediction

This theory is compared directly with a Cowell orbital prediction program without the application of a numerical fitting procedure. To produce a meaningful and convenient comparison, the following approach is used. For a chosen set of initial averaged orbital elements, the associated osculating state vectors are determined from the transformation, Eqs. (3). These, together with the initial ballistic coefficients, are then treated as the initial conditions to generate a reference ephemeris using the numerical integration program. At each data point, the ephemeris is transformed to the averaged orbital elements using the transformation for comparison. In order to examine the most severe drag effects and to minimize significant truncation and roundoff errors, only the simulated satellite cases with lifetime less than forty days are included in this study. The comparisons are made from epoch time until the satellite altitude decreases to 90 km (the adopted Jacchia atmospheric density table has a lower bound at this altitude).

Three simulated examples, which exhibit the general characteristics observed from the test cases conducted to date, will be presented here. The initial conditions for these test cases are given in Table 1. Case A is shown in Figs. 1 and 2. In Fig. 1, the solid and dashed curves are the decay references generated by the numerical integration program for semimajor axis and eccentricity, respectively, while the dots are the predictions from the semianalytic theory. The dots are not equally spaced since automatic step size is used in integration. To illustrate the differences between the two on a much smaller scale, the deviations at common time points are shown in Fig. 2. The subscript N appearing in the figures stands for the value obtained from the numerical integration

Table 1 Initial conditions for test cases A,B, and C

	A	B	C
a_{m0}, km	6665.10	6690.60	6800.00
e_{m0}	0.0061	0.0151	0.0400
i_{m0}, deg	89.98	81.98	30.00
Ω_{m0}, deg	221.40	353.80	0.00
ω_{m0}, deg	139.00	32.20	0.00
M_{m0}, deg	0.00	0.00	0.00
B, m^2/kg	0.0181	0.0172	0.0160
t_0	4/15/59	10/17/62	10/18/78

Table 2 Lifetime comparisons

	Numerical integrations, days	Semianalytic theory, days	Percentage difference, %
Case A	11.940	11.948	+0.06
Case B	35.016	34.827	−0.54
Case C	5.376	5.327	−0.91

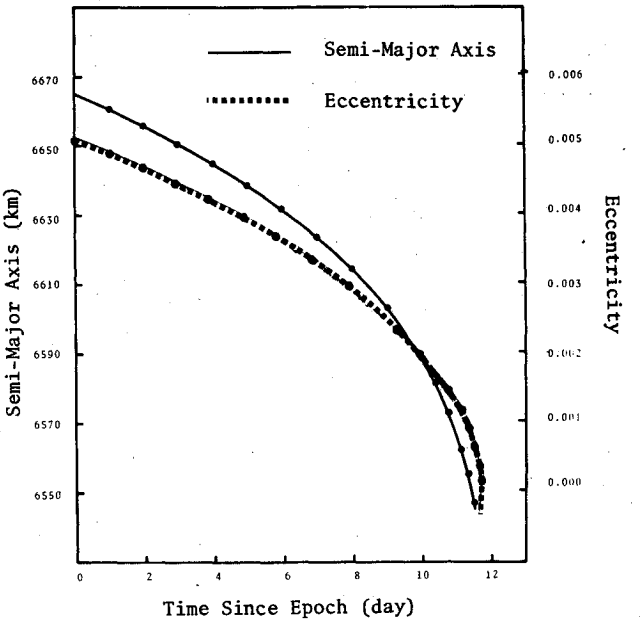

Fig. 1 Semimajor axis and eccentricity vs time (case A).

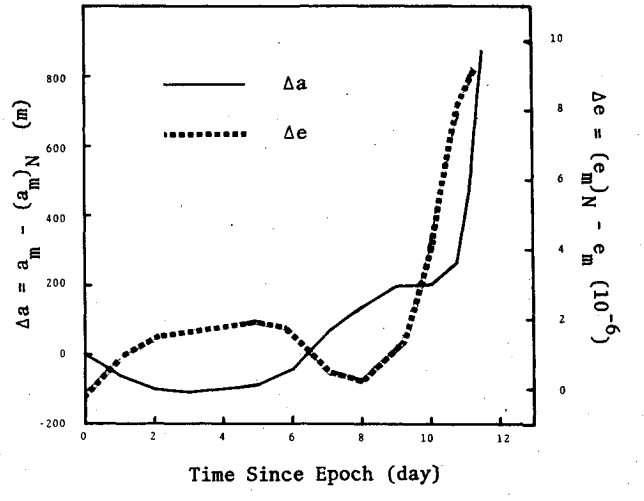

Fig. 2 Δa and Δe vs time (case A).

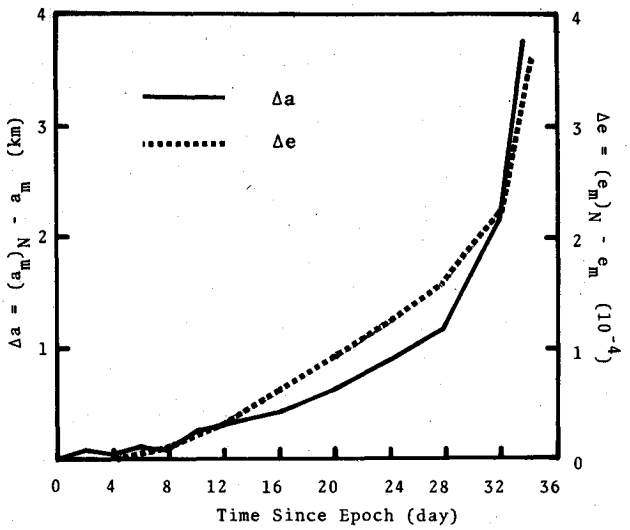

Fig. 3 Δa and Δe vs time (case B).

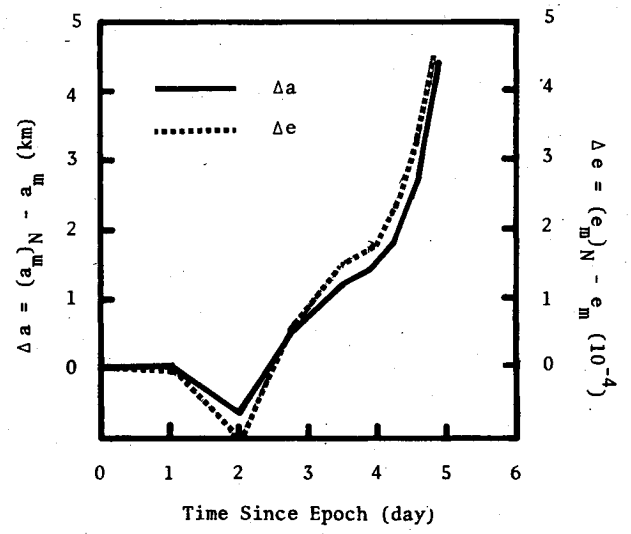

Fig. 4 Δa and Δe vs time (case C).

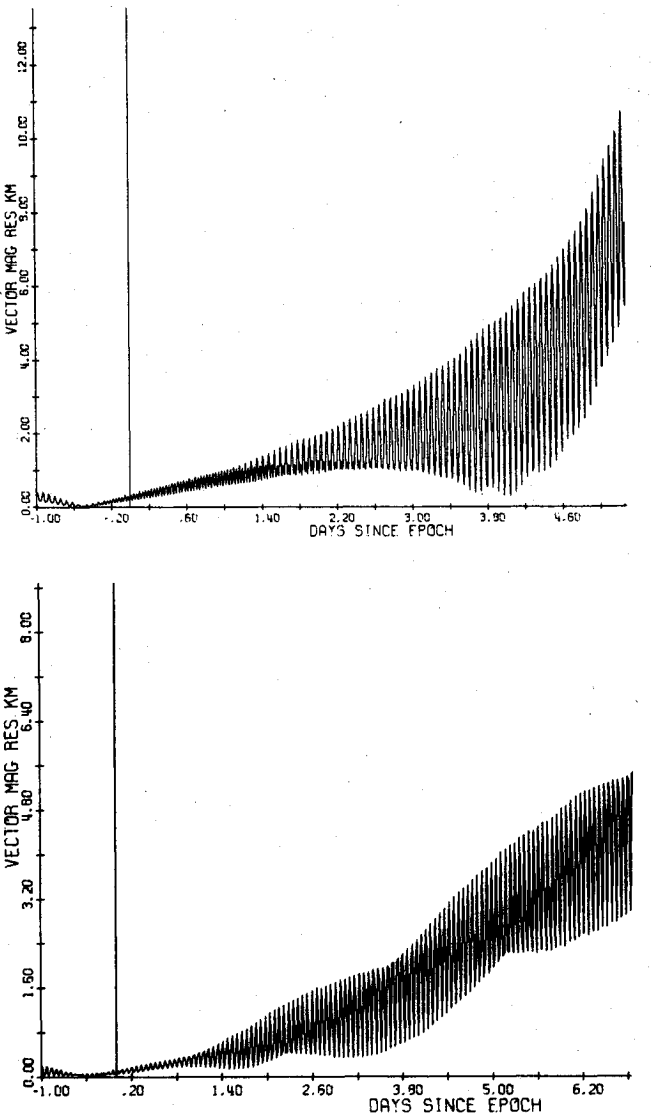

Fig. 5 Vector magnitude residual vs time (top—case D, bottom—case E).

Table 3 Initial conditions for test cases D and E

	D	E
x_0, km	−3872.4357	5600.5056
y_0, km	−5266.8818	−114.75407
z_0, km	−4876.8431	3480.5525
$\dot{x}_0$, km/s	2.9730697	−4.5310470
$\dot{y}_0$, km/s	−1.5269256	1.3693933
$\dot{z}_0$, km/s	−7.1095299	6.5604594
B, m^2/kg	0.01761	0.01720
t_0	9/3/62	10/17/62
$F_{10.7}$	85	83
$\bar{F}_{10.7}$	85	83
a_p	8	8

Table 4 Epoch mean elements for test cases D and E

	D	E
a_{m0}, km	6637.754	6688.822
e_{m0}	0.0131723	0.014825
i_{m0}, deg	65.2192	81.9799
Ω_{m0}, deg	48.1063	352.6351
ω_{m0}, deg	184.3247	28.6000
M_{m0}, deg	331.0118	268.2839
B, m^2/kg	0.01761958	0.01721699
t_0	9/3.993056/62	10/17.993056/62

program. The results for cases B and C are shown in Figs. 3 and 4, respectively. The lifetimes for these simulated satellites are shown in Table 2. The values for $F_{10.7}$, $\bar{F}_{10.7}$, and a_p are given as functions of time. Their particular values at any given time are obtained by linear interpolation. For all three cases, thirteen points were used in the quadrature evaluation for the drag effects. With the use of a second-order transformation, as discussed earlier, the predictions are expected to be improved.

Short-Term Prediction

For short-term predictions, the satellite instantaneous position is of great interest and an appropriate numerical fitting procedure is necessary to determine the initial condition for accurate prediction. To perform this numerical examination, a precision, special perturbation program (an eighth-order Gauss-Jackson integrator with variable integration step size) is used to generate reference orbits in osculating state. A number of test cases have been examined and two test cases are given here for illustration. The initial conditions and reference parameters for the test cases can be found in Table 3.

A least-squares, seven-element, differential correction algorithm is then used to determine the initial conditions for the semianalytic theory to best fit the reference orbit backward over one day. The epoch and the initial conditions are then placed at the end of the fitting span for the predictions.

Comparisons are made throughout the prediction interval for in-track, cross-track, radial, and total position vector magnitude differences. Here, in-track is, in the sense, perpendicular to the position vector and points to the direction of motion, while radial, in-track and cross-track formulate a right-handed system. To simplify the procedure, constant values for $F_{10.7}$, $\bar{F}_{10.7}$, and a_p have been assumed. The fitted initial conditions for the semianalytic theory are illustrated in Table 4.

Only the total vector magnitude differences will be shown in the paper. Figure 5 (top) illustrates case D which includes one day initial orbit determination and five days prediction. The vertical line in the figure separates the orbit determination and prediction intervals. Figure 5 (bottom) shows the results for case E, except that it includes six and one half days prediction. For both cases, seventeen points were used for the quadrature evaluations. It should be noted that the prediction accuracy is not only a function of the degree of exactness of the ephemeris theory, but also is a function of the orbit determination interval, the accuracy of the data available, and their distribution within the time interval. Should any one of the above-mentioned items vary, the predictions will also vary accordingly.

Conclusions

It has been demonstrated that accurate long- and short-term predictions using the semianalytic theory presented here can be obtained if proper initialization procedures are used. It should be noted that the results obtained thus far are generated from the simplified averaged equations of motion, Eqs. (6), to save computation time. If the equations of motion, Eqs. (4), are to be used in their entirety, some improvement in accuracy may be expected. For cases with large eccentricity and high altitude, additional significant perturbative forces should be included. This theory is formulated so that additional perturbative forces can be included readily using the various existing solutions in literature, obtained by using a method of averaging or an equivalent perturbation technique.

Appendix A: First-Order Short-Periodic Variations

$$a_{sp} = J_2\left(\frac{R^2}{a}\right)\left\{\left(\frac{a}{r}\right)^3\left[1-\frac{3}{2}\sin^2 i+\frac{3}{2}\sin^2 i\cos 2(\omega+f)\right]-\left(1-\frac{3}{2}\sin^2 i\right)(1-e^2)^{-3/2}\right\}$$

$$e_{sp} = \frac{1}{2}J_2\left(\frac{R}{p}\right)^2\left(1-\frac{3}{2}\sin^2 i\right)\left\{\frac{1}{e}\left[1+\frac{3}{2}e^2-(1-e^2)^{3/2}\right]+3\left(1+\frac{e^2}{4}\right)\cos f+\frac{3}{2}e\cos 2f+\frac{e^2}{4}\cos 3f\right\}$$

$$+\frac{3}{8}J_2\left(\frac{R}{p}\right)^2\sin^2 i\left[\left(1+\frac{11}{4}e^2\right)\cos(2\omega+f)+\frac{e^2}{4}\cos(2\omega-f)+5e\cos(2\omega+2f)\right.$$

$$\left.+\frac{1}{3}\left(7+\frac{17}{4}e^2\right)\cos(2\omega+3f)+\frac{3}{2}e\cos(2\omega+4f)+\frac{e^2}{4}\cos(2\omega+5f)+\frac{3}{2}e\cos 2\omega\right]$$

$$i_{sp} = \frac{3}{8}J_2\left(\frac{R}{p}\right)^2\sin 2i\left[e\cos(2\omega+f)+\cos 2(\omega+f)+\frac{e}{3}\cos(2\omega+3f)\right]$$

$$\omega_{sp} = \frac{3}{4}J_2\left(\frac{R}{p}\right)^2(4-5\sin^2 i)(f-M+e\sin f)+\frac{3}{2}J_2\left(\frac{R}{p}\right)^2\left(1-\frac{3}{2}\sin^2 i\right)\left[\frac{1}{e}\left(1-\frac{1}{4}e^2\right)\sin f+\frac{1}{2}\sin 2f+\frac{1}{12}e\sin 3f\right]$$

$$-\frac{3}{2}J_2\left(\frac{R}{p}\right)^2\left\{\frac{1}{e}\left[\frac{1}{4}\sin^2 i+\frac{e^2}{2}\left(1-\frac{15}{8}\sin^2 i\right)\right]\sin(2\omega+f)+\frac{e}{16}\sin^2 i\sin(2\omega-f)\right.$$

$$+\frac{1}{2}\left(1-\frac{5}{2}\sin^2 i\right)\sin 2(\omega+f)-\frac{1}{e}\left[\frac{7}{12}\sin^2 i-\frac{e^2}{6}\left(1-\frac{19}{8}\sin^2 i\right)\right]\sin(2\omega+3f)$$

$$\left.-\frac{3}{8}\sin^2 i\sin(2\omega+4f)-\frac{1}{16}e\sin^2 i\sin(2\omega+5f)\right\}-\frac{9}{16}J_2\left(\frac{R}{p}\right)^2\sin^2 i\sin 2\omega$$

$$\Omega_{sp} = -\frac{3}{2}J_2\left(\frac{R}{p}\right)^2\cos i\left[f-M+e\sin f-\frac{e}{2}\sin(2\omega+f)-\frac{1}{2}\sin 2(\omega+f)-\frac{e}{6}\sin(2\omega+3f)\right]$$

$$M_{sp} = -\frac{3}{2}J_2\left(\frac{R}{p}\right)^2\frac{\sqrt{1-e^2}}{e}\left\{\left(1-\frac{3}{2}\sin^2 i\right)\left[\left(1-\frac{1}{4}e^2\right)\sin f+\frac{e}{2}\sin 2f+\frac{e^2}{12}\sin 3f\right]+\frac{1}{2}\sin^2 i\left[-\frac{1}{2}\left(1+\frac{5}{4}e^2\right)\sin(2\omega+f)\right.\right.$$

$$\left.\left.-\frac{e^2}{8}\sin(2\omega-f)+\frac{7}{6}\left(1-\frac{e^2}{28}\right)\sin(2\omega+3f)+\frac{3}{4}e\sin(2\omega+4f)+\frac{e^2}{8}\sin(2\omega+5f)\right]\right\}+\frac{9}{16}J_2\left(\frac{R}{p}\right)^2\sqrt{1-e^2}\sin^2 i\sin 2\omega$$

$$r_{sp} = -\frac{1}{2}J_2\left(\frac{R^2}{p}\right)\left(1-\frac{3}{2}\sin^2 i\right)\left[1+\frac{e}{1+\sqrt{1-e^2}}\cos f+\frac{2}{\sqrt{1-e^2}}\left(\frac{r}{a}\right)\right]+\frac{1}{4}J_2\left(\frac{R^2}{p}\right)\sin^2 i\cos(2\omega+2f)$$

Appendix B: Averaged Variational Equations Due to J_2, J_3, J_4

$$\langle \dot{a}_G \rangle = 0$$

$$\langle \dot{e}_G \rangle = -\frac{3}{32}nJ_2^2\left(\frac{R}{p}\right)^4\sin^2 i(14-15\sin^2 i)e(1-e^2)\sin 2\omega-\frac{3}{8}nJ_3\left(\frac{R}{p}\right)^3\sin i(4-5\sin^2 i)(1-e^2)\cos\omega$$

$$-\frac{15}{32}nJ_4\left(\frac{R}{p}\right)^4\sin^2 i(6-7\sin^2 i)e(1-e^2)\sin 2\omega$$

$$\langle(\dot{i})_G\rangle = \frac{3}{64}nJ_2^2\left(\frac{R}{p}\right)^4 \sin 2i(14-15\sin^2 i)e^2\sin 2\omega + \frac{3}{8}nJ_3\left(\frac{R}{p}\right)^3 \cos i(4-5\sin^2 i)e\cos\omega$$

$$+\frac{15}{64}nJ_4\left(\frac{R}{p}\right)^4 \sin 2i(6-7\sin^2 i)e^2\sin 2\omega$$

$$\langle\dot{\omega}_G\rangle = \frac{3}{4}nJ_2\left(\frac{R}{p}\right)^2(4-5\sin^2 i) + \frac{3}{16}nJ_2^2\left(\frac{R}{p}\right)^4\left\{48-103\sin^2 i+\frac{215}{4}\sin^4 i\right.$$

$$+\left(7-\frac{9}{2}\sin^2 i-\frac{45}{8}\sin^4 i\right)e^2+6\left(1-\frac{3}{2}\sin^2 i\right)(4-5\sin^2 i)\sqrt{1-e^2}-\frac{1}{4}\left[2(14-15\sin^2 i)\sin^2 i-(28\right.$$

$$\left.\left.-158\sin^2 i+135\sin^4 i)e^2\right]\cos 2\omega\right\}+\frac{3}{8}nJ_3\left(\frac{R}{p}\right)^3\left[(4-5\sin^2 i)\frac{\sin^2 i-e^2\cos^2 i}{e\sin i}\right.$$

$$\left.+2\sin i(13-15\sin^2 i)e\right]\sin\omega-\frac{15}{32}nJ_4\left(\frac{R}{p}\right)^4\left\{16-62\sin^2 i+49\sin^4 i\right.$$

$$\left.+\frac{3}{4}(24-84\sin^2 i+63\sin^4 i)e^2+\left[\sin^2 i(6-7\sin^2 i)-\frac{1}{2}(12-70\sin^2 i+63\sin^4 i)e^2\right]\cos 2\omega\right\}$$

$$\langle\dot{\Omega}_G\rangle = -\frac{3}{2}nJ_2\left(\frac{R}{p}\right)^2\cos i-\frac{3}{2}nJ_2^2\left(\frac{R}{p}\right)^4\cos i\left[\frac{9}{4}+\frac{3}{2}\sqrt{1-e^2}-\sin^2 i\left(\frac{5}{2}+\frac{9}{4}\sqrt{1-e^2}\right)+\frac{e^2}{4}\left(1+\frac{5}{4}\sin^2 i\right)\right.$$

$$\left.+\frac{e^2}{8}(7-15\sin^2 i)\cos 2\omega\right]-\frac{3}{8}nJ_3\left(\frac{R}{p}\right)^3(15\sin^2 i-4)e\cot i\sin\omega$$

$$+\frac{15}{16}nJ_4\left(\frac{R}{p}\right)^4\cos i\left[(4-7\sin^2 i)\left(1+\frac{3}{2}e^2\right)-(3-7\sin^2 i)e^2\cos 2\omega\right]$$

$$\langle\dot{M}_G\rangle = n\left[1+\frac{3}{2}J_2\left(\frac{R}{p}\right)^2\left(1-\frac{3}{2}\sin^2 i\right)\sqrt{1-e^2}\right]+\frac{3}{2}nJ_2^2\left(\frac{R}{p}\right)^4\left\{\left(1-\frac{3}{2}\sin^2 i\right)^2(1-e^2)\right.$$

$$+\left[\frac{5}{4}\left(1-\frac{5}{2}\sin^2 i+\frac{13}{8}\sin^4 i\right)+\frac{5}{8}\left(1-\sin^2 i-\frac{5}{8}\sin^4 i\right)e^2\right.$$

$$\left.\left.+\frac{1}{16}\sin^2 i(14-15\sin^2 i)\left(1-\frac{5}{2}e^2\right)\cos 2\omega\right]\sqrt{1-e^2}\right\}$$

$$+\frac{3}{8}nJ_2^2\left(\frac{R}{p}\right)^4\frac{1}{\sqrt{1-e^2}}\left\{3\left[3-\frac{15}{2}\sin^2 i+\frac{47}{8}\sin^4 i+\left(\frac{3}{2}-5\sin^2 i+\frac{117}{16}\sin^4 i\right)e^2\right.\right.$$

$$\left.-\frac{1}{8}\left(1+5\sin^2 i-\frac{101}{8}\sin^4 i\right)e^4\right]+\frac{e^2}{8}\sin^2 i\left[70-123\sin^2 i+(56-66\sin^2 i)e^2\right]\cos 2\omega+\frac{27}{128}e^4\sin^4 i\cos 4\omega\right\}$$

$$-\frac{3}{8}nJ_3\left(\frac{R}{p}\right)^3\sin i(4-5\sin^2 i)\frac{1-4e^2}{e}\sqrt{1-e^2}\sin\omega$$

$$-\frac{45}{128}nJ_4\left(\frac{R}{p}\right)^4(8-40\sin^2 i+35\sin^4 i)e^2\sqrt{1-e^2}$$

$$+\frac{15}{64}nJ_4\left(\frac{R}{p}\right)^4\sin^2 i(6-7\sin^2 i)(2-5e^2)\sqrt{1-e^2}\cos 2\omega$$

Acknowledgments

The authors wish to thank their colleagues, D. Raney and G.E. Townsend of Northrop Services, Inc., for their support and many technical discussions over the initial phases of this research. The authors are grateful to D.R. Larson and R.S. Hujsak for their efforts in implementing the theory in the ADCOM software system which made the short-term prediction study possible. The initial phase of this research was originated at Northrop Services, Inc., Huntsville, Ala. and supported by NASA-MSFC under Contract NAS8-21810.

References

[1] Brouwer, D. and Hori, G., "Theoretical Evaluation of Atmospheric Drag Effects in the Motion of an Articifical Satellite," *Astronomical Journal,* Vol. 66, June 1961, pp. 193-225.

[2] Lane, M.H., "The Development of an Artificial Satellite Theory Using a Power-Law Atmospheric Density Representation," AIAA Paper 65-35, AIAA 2nd Aerospace Sciences Meeting, New York, Jan. 1965.

[3] Lane, M.H., Fitzpatrick, P.M., and Murphy J.J., "On the Representation of Air Density in Satellite Deceleration Equations by Power Functions with Integral Exponents," Project SPACETRACK, Air Proving Ground Center, Eglin AFB, Fla., Tech. Doc. Rept. No. APGC-TDR-62-15, March 1962.

[4] Lane, M.H. and Cranford, K.H., "An Improved Analytical Drag Theory for the Artificial Satellite Problem," AIAA Paper 69-925, AIAA/AAS Astrodynamics Conference, Princeton, N.J., Aug. 20-22, 1969.

[5] Hoots, F.R., "Theory of the Motion of an Artificial Satellite," Analysis Memo 79-1, ADCOM/DO6, Peterson AFB, Colo., (to be published in *Celestial Mechanics*).

[6] Brouwer, D., "Solution of the Problem of Artificial Satellite Theory Without Drag," *Astronomical Journal,* Vol. 64, Nov. 1959, pp. 378-397.

[7] Lyddane, R.H., "Small Eccentricities or Inclinations in the Brouwer Theory of the Artificial Satellite," *Astronomical Journal,* Vol. 68, Oct. 1963, pp. 555-558.

[8] Zee, C.H., "Trajectories of Satellites Under the Combined Influences of Earth Oblateness and Air Drag," *Celestial Mechanics,* Vol. 3, March 1971, pp. 148-168.

[9] Chen, S.C.H., "Ephemeris Generation for Earth Satellites Considering Earth Oblateness and Atmospheric Drag," Northrop Services, Inc., Huntsville Ala., M-240-1239, May 1974.

[10] Mueller, A.C., "Atmospheric Density Models," Analytical and Computational Mathematics, Inc., Houston, Tx., ACM-TR-106, June 1977.

[11] Mueller, A., Scheifele, G., and Starke, S., "An Analytical Orbit Prediction for Near-Earth Satellites," AIAA Paper 79-122, 17th Aerospace Sciences Meeting, New Orleans, La., Jan. 1979.

[12] Pimm, R.S., "Long-Term Orbital Trajectory Determination by Superposition of Gravity and Drag Perturbations," AAS Paper 71-376, AAS/AIAA Astrodynamics Specialist Conference, Ft. Lauderdale, Fla., Aug. 17-19, 1971.

[13] Small, H.W., "The Motion of a Satellite About an Oblate Earth," Lockheed Missiles and Space Co., Tracking Note No. 4, LMSC-A086756, 1961.

[14] Kaufman, B. and Dasenbrock, R., "Long Term Stability of Earth and Lunar Orbits: Theory and Analysis," AIAA Paper 72-936, AIAA/AAS Astrodynamics Conference, Palo Alto, Calif., Sept. 11-12, 1972.

[15] Cefola, P.J., Long, A.C., and Holloway, G., Jr., "The Long-Term Prediction of Artificial Satellite Orbit," AIAA Paper 74-170, 12th Aerospace Sciences Meeting, Washington, D.C., Jan. 1974.

[16] McClain, W.D., Long, A.C., and Early, L.W., "Development and Evaluation of a Hybrid Averaged Orbit Generator," AIAA Paper 78-1382, AIAA/AAS Astrodynamics Conference, Palo Alto, Calif., Aug. 1978.

[17] Hujsak, R.S., "A Restricted Four Body Solution for Resonating Satellites with an Oblate Earth," AIAA Paper 79-136, AAS/AIAA Astrodynamics Specialist Conference, Provincetown, Ma., June 1979.

[18] Liu, J.J.F., "Satellite Motion About an Oblate Earth," *AIAA Journal,* Vol. 12, Nov. 1974, pp. 1511-1516.

[19] Liu, J.J.F. and Alford, R.L., "An Introduction to Gauss-Legendre Quadrature," Northrop Services, Inc., Huntsville Ala., M-240-1288, Oct. 1973.

[20] Alford, R.L. and Liu, J.J.F., "The Orbital Decay and Lifetime (LIFTIM) Prediction Program," Northrop Services, Inc., Hunstville Ala., M-240-1278, May 1974.

[21] Liu, J.J.F., "Satellite Motion About an Oblate Earth With Drag," Northrop Services, Inc., Huntsville Ala., TN-240-1383, Feb. 1975.

[22] Kyner, W.T., "Averaging Method in Celestial Mechanics," *The Theory of Orbits in the Solar System and in Stellar System,* edited by G. Contopoulous, Academic Press, London and New York, 1966.

[23] Liu, J.J.F., "Certain Comments on the Method of Averaging and Its Applications," Northrop Services, Inc., Huntsville, Ala., TN-242-1045, Jan. 1972.

[24] Liu, J.J.F. and Alford, R.L., "A Semi-Analytic Theory for the Motion of a Close-Earth Artificial Satellite With Drag," AIAA Paper 79-0123, 17th Aerospace Sciences Meeting, New Orleans, La., Jan. 1979.

[25] *Models of Earth's Atmosphere (90 to 2500 km),* NASA SP-8021, March 1973.

[26] Jacchia, L.G., "New Static Models of the Thermosphere and Exosphere With Empirical Temperature Profiles," Smithsonian Astrophysical Observatory, SP-313, May 1970.

[27] Lyddane, R.H. and Cohen, C.J., "Numerical Comparison Between Brouwer's Theory and Solution by Cowell's Method for the Orbit of an Artificial Satellite," *Astronomical Journal,* Vol. 67, April 1962, pp. 176-177.

[28] Breakwell, J.V. and Vagners, J., "On Error Bounds and Initialization in Satellite Orbit Theories," *Celestial Mechanics,* Vol. 2, 1970, pp. 253-264.